BMC Veterinary Research

RESEARCH

Open Access

Host susceptibilities and entry processes of SARS-CoV-2 Omicron variants using pseudotyped viruses carrying spike protein

Alexandria Zabiegala[1], Yunjeong Kim[1] and Kyeong-Ok Chang[1*]

Abstract

The zoonotic potential has been well studied for SARS-CoV-2 and its earlier variants, but the information for Omicron variants and SARS-CoV is lacking. In this study, we generated lentivirus-based pseudoviruses carrying spike protein (S) of SARS-CoV-2, parental and Omicron variants including BA.1.1, BA.4/5, XBB.1 and JN.1 to assess the entry into cells expressing human or animal ACE2 including dogs, cats and white-tailed deer. Using these pseudoviruses, along with pseudoviruses carrying S of MERS-CoV and SARS-CoV, we assessed the protease processing of these various S through western blotting, entry/inhibition assays, and fusion assays. The results showed that overall, pseudotyped viruses carrying each S of SARS-CoV-2 Omicron strains efficiently entered cells expressing human or animal ACE2 comparably (BA.1.1 and JN.1) or better (BA.4/5 and XBB.1) than those with parental strain. In addition, the entries of pseudotyped viruses carrying S of SARS-CoV were also efficient the cells expressing human or animal ACE2. The presence of TMPRSS2 significantly increased the entry of all tested pseudoviruses including those with S of MERS-CoV, SARS-CoV and SARS-CoV-2, with BA.1.1, JN1, and XBB.1 Omicron having the largest fold increase. When cathepsin inhibitors were examined to assess their inhibitory effects on entry of parental and Omicron variants, they were significantly less effective in the entry of Omicron variants compared to parent strain, suggesting Omicron strains do not depend on the endosomal route compared to parental strain.

Keywords Coronavirus, SARS-CoV, SARS-CoV-2, Spike, ACE2, TMPRSS2, Pseudovirus assay

Introduction

Coronaviruses are enveloped viruses that have a single stranded, positive-sense RNA genome in the *Coronaviridae* family. Many coronaviruses cause diverse diseases in a wide range of animals, including humans. Novel coronaviruses have periodically surfaced in human populations from animal to human spillover events, which include severe acute respiratory syndrome coronavirus (SARS-CoV), Middle Eastern Respiratory Syndrome coronavirus (MERS-CoV) and most recently SARS-related coronavirus 2 (SARS-CoV-2). SARS-CoV outbreaks that occurred in 2003 caused severe respiratory illness and spread from China to more than a dozen countries [1] before it was no longer reported since 2004 [2]. MERS-CoV was first reported in Saudi Arabia in 2012 and has been mainly found in countries in and near the Arabian Peninsula with occasional outbreaks outside the Middle East [3]. MERS-CoV transmission is mainly by direct or indirect contact with dromedary camels with limited person-to-person transmission [3]. SARS-CoV and MERS-CoV have mortality rates of approximately 13% and 35%, respectively [4–6]. In late 2019,

*Correspondence:
Kyeong-Ok Chang
kchang@vet.ksu.edu
[1]Department of Diagnostic Medicine and Pathobiology, College of Veterinary Medicine, Kansas State University, 1800 Denison Avenue, Manhattan, KS 66506, USA

another novel coronavirus, SARS-CoV-2 unexpectedly emerged [7]. Coronavirus disease (COVID-19), caused by SARS-CoV-2, is a mild to severe respiratory illness with an increased mortality in populations with underlying health conditions or of advanced ages [8, 9]. Unlike its two novel coronavirus predecessors, SARS-CoV-2 has rapidly spread worldwide resulting in the World Health Organization's declaration of the COVID-19 pandemic in March 2020. Since the first report of SARS-CoV-2, multiple antigenically distinct variants have emerged over the years, each time eventually replacing earlier variants. Compared to the parental reference Wuhan-Hu-1 strain, the Omicron variants have more than 30 mutations on the spike protein (S) and at least 15 mutations in the receptor-binding domain (RBD), which is substantially more than other variants of concern [10]. The Omicron variant has continuously evolved since the emergence of the first dominant variant BA.1 (B.1.1.529.1) in late 2021 [11] and is composed of several major sub-lineages BA.1.1 (B.1.1.529.1.1), BA.2 (B.1.1.529.2), BA.3 (B.1.1.529.3), BA.4/5 (B.1.1.529.4/ B.1.1.529.5) and their recombinant variants such as XBB [12, 13]. JN.1, a more recent variant which was first detected in August of 2023 [14], was the most prominent strain in the beginning of 2024 [15, 16]. As of January 2025, the main SARS-CoV-2 circulating strains are descendants of the JN.1 subvariant [17].

Viral entry into host cells plays a key role in host susceptibility and tissue tropism. With SARS-CoV and SARS-CoV-2, the virus-cell interaction occurs between the spike protein (S) and the cell receptor angiotensin converting enzyme-2 (ACE2). Coronavirus S forms a trimer, and each monomeric S is composed of two parts, the S1 and S2 subunits. The S1 subunit contains the receptor binding domain (RBD) that directly interacts with ACE2, and the S2 subunit has the hydrophobic fusion peptide at the S2' site, which is implicated in viral fusion and entry. SARS-CoV-2 S has polybasic amino acids at the S1/S2 junction, which is subjected to cleavage by furin by the parental cell prior to release (reviewed in [18]). The polybasic cleavage site at the S1/S2 junction found in SARS-CoV-2, but not in SARS-CoV, has been implicated in increasing cleavage and virus transmissibility (reviewed in [18]), likely due to a more accessible RBD to ACE2 [19]. During viral circulation, the S protein can adopt an "open" or "closed" position where the RBD is only accessible in the "open" position for binding of ACE2 or antibodies targeting the RBD [20, 21]. Conformational change in the S following receptor binding allows S2' site cleavage by cellular proteases, such as transmembrane serine protease 2 (TMPRSS2), which exposes the fusion peptide to the cell membrane for direct fusion [22–26]. Previous research demonstrated that SARS-CoV-2 enters cells via two distinct routes: when TMPRSS2 is present on the cell membrane, SARS-CoV-2 preferentially utilizes a direct entry route by fusion of the viral envelope to the cellular membrane, but in the absence of this protease, SARS-CoV-2 enter cells via an endosomal entry route where proteolytic processing of S is mediated by cathepsins [27]. These two distinct routes have also been described for SARS-CoV [28] and MERS-CoV [29].

As it became evident that SARS-CoV-2 was a global health threat, identification of animal species that are susceptible to this virus infection has become important to find potential animal reservoirs, which led to extensive research on the zoonotic risk of domestic and wild animals. Previous research has shown that many species are susceptible to SARS-CoV-2 infection in experimental settings and/or naturally, with or without clinical signs or virus shedding. Additionally, some animal species including white-tailed deer, mink and hamsters have demonstrated animal-to-animal virus transmission [12, 13]. A summary of the data on experimental and natural infections can be found in the supplementary materials (Supplementary Table 1). We and others have previously reported that SARS-CoV-2 interacts with ACE2 from various animal species using lentivirus-based pseudoviruses carrying the spike protein(S) of various SARS-2 strains and cells stably expressing animal ACE2 [18, 30]. The animal ACE2s used in this study include human, horse, dog, cat, Syrian golden hamster, mink, white-tailed deer, bovine, and dromedary camel. As these studies have mainly focused on parental or earlier variants, in this study, we examined whether the mutations in the S of SARS-CoV-2 BA.1.1, BA.4/5, JN.1, or XBB.1 Omicron subvariants change viral entry efficiency in cells expressing animal ACE2 compared to their infectivity of cells expressing human ACE2. We hypothesize that high rates of mutations present in S gene of Omicron subvariants significantly affect their binding capabilities and entries to the cells expressing various animal ACE2. We also examined the entry of pseudovirus carrying SARS-CoV S, which also utilizes ACE2 as the receptor, in these cell lines. To investigate the differences in protease activity on S of SARS-CoV, MERS-CoV, and SARS-CoV-2 parental and Omicron subvariants, we performed western blots of concentrated pseudoviruses, entry assays of the pseudoviruses into cells expressing the appropriate functional receptor (ACE2 for SARS-CoV and SARS-CoV-2 S and DPP4 for MERS-CoV S) with or without TMPRSS2, and fusion studies of each parental S and its respective functional receptor with or without TMPRSS2.

Materials and methods

Cells and plasmids

Human embryonic kidney 293T (HEK293T)(#CRL-3216) and Crandell-Rees feline kidney (CRFK)(#CCL-94) cells were purchased from American Type Culture

Collection (ATCC; Manassas, VA) and maintained in Dulbecco's Modified Eagle Medium (DMEM) or Eagle's Minimal Essential Medium (MEM) supplemented with 10% or 5% fetal bovine serum respectively, 100 U/ml penicillin and 100 µg/ml streptomycin. Generation of the CRFK cells stably expressing ACE2 from human, horse, dog, cat, Syrian golden hamster, mink, white-tailed deer, bovine and dromedary camel was previously reported by our lab [30]. Generation of the plasmid expressing the S of SARS-CoV-2 parental strain, designated as pAbVec-SARS2-S, was also reported by us [30]. The plasmids expressing the S of SARS-CoV (#pCVM3-SARS-CoV-S, (#VG40150-G-N), MERS-CoV(#VG40069-CF), Omicron BA.1.1 (VG40986-UT), Omicron XBB.1 (#VG40978-UT), and Omicron JN.1 (#VG40986-UT) subvariants were purchased from Sino Biologicals (Wayne, PA) and the plasmid expressing Omicron BA.4/5 was obtained from InvivoGen (#p1-spike-v13, San Diego, CA). The mutations found in the RBD of SARS-CoV-2 Omicron variants compared to parental SARS-CoV-2 RBD [31–33] are shown in Table 1. The plasmids carrying S of MERS-CoV or HCoV-EMC/2012 were cloned into the pSI plasmid after the full-length, codon-optimized S gene of each virus was synthesized from Integrated DNA technology (Coralville, IA) for this study.

Table 1 Mutations found in the RBD of SARS-CoV-2 Omicron variants compared to parental SARS-CoV-2 RBD. Mutations found in all four Omicron strains are indicated by bolded text, and residues that form hydrogen bonds between parental SARS-CoV-2 parental S and human ACE2 are italic

Omicron BA.1.1	Omicron BA.4/5	Omicron JN.1	Omicron XBB
G339D	G339D	I332V	G339H
R346K	S371F	G339H	R346T
S371L	S373P	K356T	L368I
S373P	S375F	S371F	S371F
S375F	T376A	S373P	S373P
K417N	D405N	S375F	S375F
N440K	R408S	T376A	T376A
G446S	K417N	R403K	D405N
S477N	N440K	D405N	R408S
T478K	L452R	R408S	K417N
E484A	S477N	K417N	N440K
Q493R	T478K	N440K	V445P
G496S	E484A	V445H	G446S
Q498R	F486V	G446S	N460K
N501Y	Q498R	N450D	S477N
Y505H	N501Y	L452W	T478K
	Y505H	L455S	E484A
		N460K	F486S
		S477N	F490S
		T478K	Q498R
		N481K	N501Y
		Δ483	Y505H
		E484K	
		F486P	
		Q498R	
		N501Y	
		Y505H	

Generation of pseudoviruses

Pseudotyped viruses containing the S genes of interest were generated using a second-generation lentiviral packaging system with a packaging plasmid psPAX2 (#12260, Addgene, Watertown, MA), a reporter plasmid pLenti-luc (#105621, Addgene, Watertown, MA), and an envelope plasmid carrying the S gene of SARS-CoV, MERS-CoV, or SARS-CoV-2 (parental, Omicron BA.1.1, BA.4/5, JN.1, or XBB.1 variant) as previously described by us [30]. Briefly, one-day old HEK293T cells in a 6-well plate were transfected with 1 ug of PsPAX2, 1 ug pLenti-luc and 100 ng to 1 ug S using Lipofectamine 2000 (#11668019, Thermo Fisher, Waltham, MA). Based on transfection efficiency with S expression, 100 ng per well was used for Omicron BA.1.1, Omicron JN.1, and Omicron XBB.1 S while 1 ug was used for SARS-CoV-2 parental and Omicron BA.4/5 S, SARS-CoV S, and MERS-CoV S. The cells were then incubated at 37 ˚C for 48 h and the supernatant containing pseudoviruses was then collected. Cell debris was removed by centrifugation at 400 x g for 10 min before storage at -80˚C. Pseudovirus titers were determined using a Lenti-X p24 Rapid Titer Kit (#632200, Takara, San Jose, CA) [30].

Western blot analysis of pseudoviruses

Western Blot analysis was performed for pseudoviruses containing the S gene of parental strain of SARS-CoV-2, SARS-CoV, and MERS-CoV, and the Omicron BA.1.1, BA.4/5, JN.1, or XBB.1 strain of SARS-CoV-2. Pseudoviruses were concentrated by ultracentrifugation with 30% sucrose cushion at 100,000 X g for 2 h. Virus pellets were resuspended at 100-fold concentrated volume, and proteins were resolved in a 10% Novex Bis-Glycin gel (#XV00100PK20, Thermo Fisher, Waltham, MA) and transferred to a nitrocellulose membrane. The membrane was incubated with convalescent human serum against SARS-CoV-2 [30] or anti-FLAG antibodies for SARS-CoV and MERS-CoV (#ab49763 Abcam Fremont, CA). Chemiluminescent signals were visualized by FOTO/Analyst Luminary/FX Systems (Fotodyne Inc, Harland, WI).

Pseudovirus entry assays

Entry efficiencies of SARS-CoV-2, parental or Omicron variants, or SARS-CoV into cells expressing animal ACE2 were evaluated and compared to the entry into cells expressing human ACE2 using the pseudovirus entry assay in CRFK cells expressing ACE2 from human, horse, dog, cat, Syrian golden hamster, mink, white-tailed deer, bovine or dromedary camel. Briefly, one-day old CRFK cells expressing each ACE2 in a 24 well plate

were transduced with the pseudoviruses carrying S of SARS-CoV, SARS-CoV-2 parental or Omicron BA.1.1, BA.4/5, JN.1, or XBB.1 subvariants and further incubated for 30 h. Cell lysates were prepared and firefly luciferase activity was determined using the luciferase reporter assay system (#E1500 and #E2920, Promega, Madison, WI) on a luminometer (GloMax® 20/20 Luminometer, Promega, Madison, WI) following the manufacturer's direction.

The effects of TMPRSS2 on the entry of the pseudovirus containing the aforementioned S genes were determined by transducing each in HEK293T cells expressing ACE2 or DPP4 with or without TMPRSS2. Briefly, one-day old HEK293T cells were transfected with pIRES-Neo-hACE2-FLAG [30] or pCMV6-hDPP4 (#RC209466, Origene, Rockville, MD) with or without pCMV6-hTMPRSS2 (#RC208677, Origene). The plasmid expressing Renilla luciferase, pRL-CMV (#E2231, Promega), was included as an expression control. The firefly luciferase activity was normalized to the Renilla luciferase activity.

Fusion assays

To assess the roles of TMPRSS2 in the S-mediated entry of SARS-CoV, parental SARS-CoV-2, or MERS-CoV, a fusion assay was performed. HEK293T cells at 70% confluency were transfected with plasmids expressing S of SARS-CoV, parental SARS-CoV-2, or MERS-CoV, and the respective functional receptor with or without TMPRSS2. For SARS-CoV and SARS-CoV-2 fusion studies, pIRES-Neo-hACE2-FLAG plasmid [30] and an aforementioned plasmid expressing S of SARS-CoV (pCVM3-SARS-CoV-S) or SARS-CoV-2 (pAb-Vec-SARS2-S) with or without the TMPRSS2 plasmid (pCMV6-hTMPRSS2) were transfected as described above. For MERS-CoV, a plasmid expressing DPP4 (pCMV6-hDPP4) and MERS-CoV S with or without the TMPRSS2 plasmid (pCMV6-hTMPRSS2) were transfected. Twenty-four hrs post-transfection, the cells were fixed in 4% paraformaldehyde, stained with Hematoxylin and Eosin (#ab2458807, Abcam), and mounted in glycerol. Images were acquired at 40x magnification using an SDL camera through a Zeiss Axiovert 200 M microscope. The number of nuclei involved in syncytia formation at 20x magnification were manually counted over 5 fields of view and the average over the 5 fields was calculated per sample.

Cathepsin inhibitor studies

Well-known cathepsin L inhibitors including MDL28170 (#M6690) and Z-FL-CHO (#219426) (both from Sigma-Aldrich, St. Louis, MO) were tested against Omicron strains compared to parental strain using the pseudovirus entry assays in CRFK cells expressing hACE2. The enzyme assay of cathepsin L inhibition was done with cathepsin L inhibitor kit from Abcam (#ab197012, Waltham, MA) per manufacturer's instruction. The cell entry inhibition assay with pseudotyped virus carrying S of SARS-CoV-2 (parental, BA.4/5, XBB.1, JN.1, and BA.1.1) was performed in CRFK cells expressing hACE as previously described [34, 35]. In this assay, the cells were incubated with DMSO (0.1%) or serial dilutions of MDL28170 or Z-FL-CHO immediately after cells were transduced with the pseudotyped virus carrying each S. After the transduction, cells were incubated for 48 h, and luciferase activities were measured. The dose-dependent inhibition curve for each compound was prepared for both enzyme and cell-based assays, and the 50% effective concentration (IC_{50} for enzyme assay and EC_{50} for cell-based assay) values were determined by GraphPad Prism software using a variable slope (GraphPad, La Jolla, CA).

Statistical analysis

Data consists of at least three independent experiments. Statistical analysis was performed using GraphPad Prism software version 9.5 (San Diego, CA). A two-tailed Wilcoxon matched-pairs signed rank test was performed to assess the change in entry of SARS-CoV, SARS-CoV-2 parental, and SARS-CoV-2 Omicron BA.1.1, BA.4/5, JN.1, and XBB.1 into the different ACE2 expressing cell lines. A one-tailed Mann-Whitney test was used to assess the effect of TMPRSS2 expression on the parental pseudoviruses when compared to the functional receptor alone and to assess the effect on TMPRSS2 expression of number of nuclei present in syncytia formation in the fusion assays.

Results

Entry efficiencies of pseudoviruses carrying S of SARS-CoV-2 Omicron strains or SARS-CoV compared to SARS-CoV-2 parental strain in cells expressing human or animal ACE2

When the entry efficiencies of SARS-CoV-2 parental strain in cells expressing animal ACE2 were compared to human ACE2, there was a significant increase in the pseudovirus entry in cells expressing horse (3.6-fold), dog (3.39-fold), cat (2.47-fold), hamster (8.93-fold), rabbit (11.39-fold), white-tailed deer (4.09-fold), and cow (3.82-fold) ACE2 compared to human ACE2. In addition, there was a significant decrease in entry into mink ACE2 (0.35-fold) and no significant difference in camel ACE2 compared to human ACE2 (Fig. 1A). For Omicron strains, cells expressing cow or camel ACE2 were highly susceptible for the entries of all four Omicron strains compared to human ACE2. On the other hand, entries of all four pseudotyped viruses carrying S were decreased in cells expressing mink ACE2 compared to human ACE2 (Fig. 1B-E). Overall, BA.4/5 and XBB.1 have similar trends as parental strain, showing there were increased

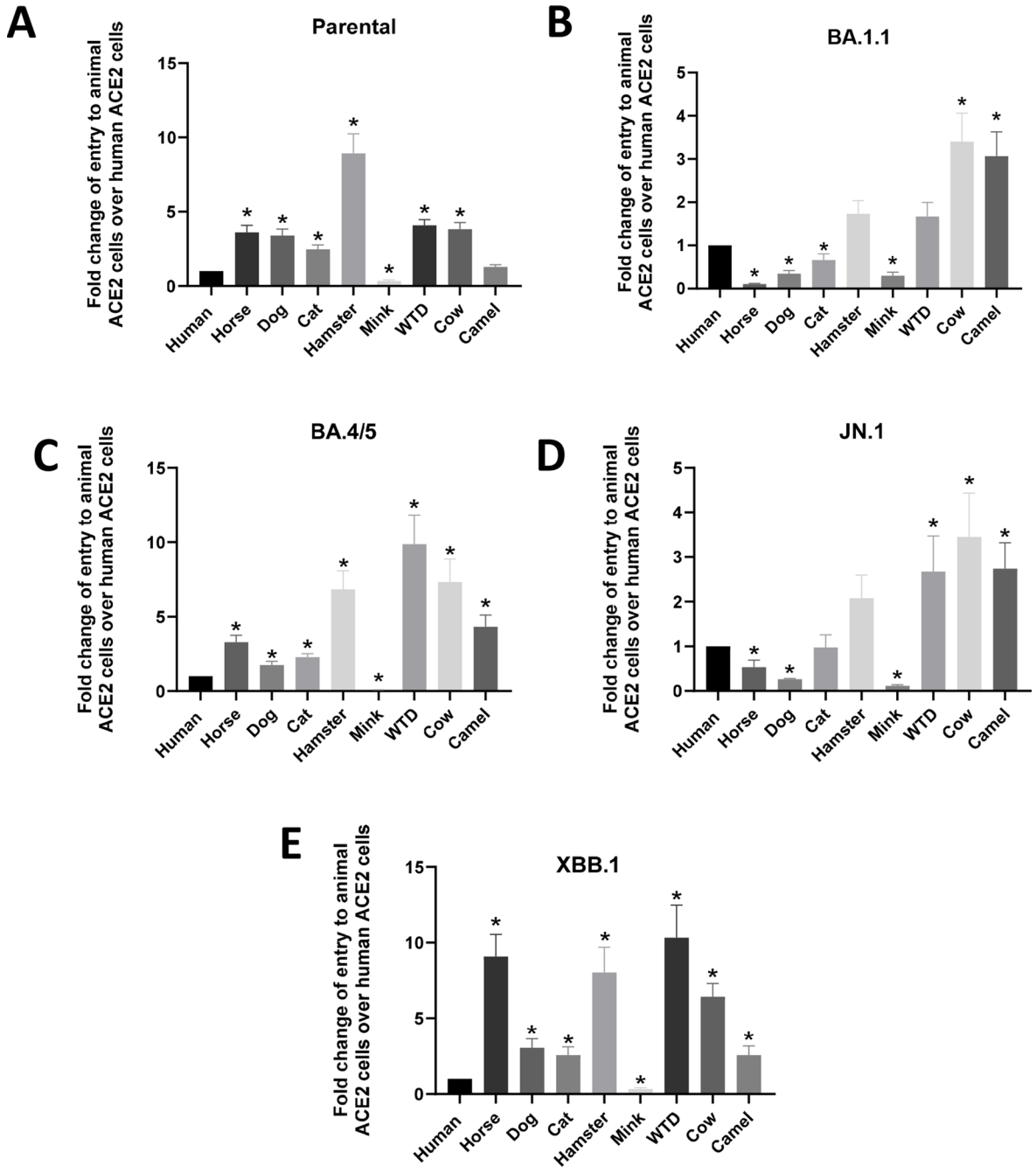

Fig. 1 Entry of pseudovirus carrying S of SARS-CoV-2 parental (**A**) or Omicron subvariants BA.1.1 (**B**), BA.4/5 (**C**), JN.1 (**D**), or XBB.1 (**E**) into cells expressing human or animal ACE2. The entry of each pseudovirus into human, horse, dog, cat, hamster, mink, white-tailed deer (WTD), cow, or camel ACE2 expressing cells was measured using a Luciferase reporter system. Fold changes of entry into cells expressing each animal ACE2 were compared to cells expressing human ACE2. Statistical differences are indicated with an asterisk (*, $P < 0.05$)

entries to horse, dog, cat, WTD, cow and camel ACE2, decreased entries to mink ACE2 compared to human ACE2 (Fig. 1C and E). For BA.1.1 and JN.1, while there were increased entries to cow and camel ACE2, there was decreased entry into cells expressing horse, dog, and mink ACE2 compared to human ACE2 (Fig. 1B and D).

The pseudoviruses carrying S of SARS-CoV efficiently entered cells expressing human or animal ACE2 at comparable levels to S of SARS-CoV-2 (Fig. 2A). When the entry efficiencies of SARS-CoV in cells expressing animal ACE2 were compared to human ACE2 (Fig. 2B), there was a significant increase of entry in dog (2.4-fold), cat (6.29-fold), hamster (6.58-fold), white-tailed deer

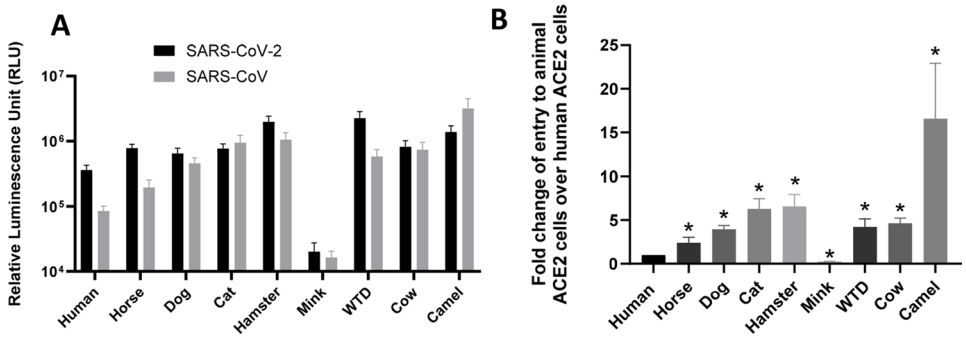

Fig. 2 Entry of pseudovirus carrying S of SARS-CoV into cells expressing human or animal ACE2. The entry of each pseudovirus into human, horse, dog, cat, hamster, mink, white-tailed deer (WTD), cow, or camel ACE2 expressing cells was measured using a Luciferase reporter system. (**A**) The relative luminescence unit (RLU) of pseudoviruses carrying S of SARS-CoV or parental SARS-CoV-2 into cells expressing human or animal ACE2. (**B**) Fold changes of entry into each cell types were compared to cells expressing human ACE2. Statistical differences are indicated with an asterisk (*, $P < 0.05$)

(4.22-fold), cow (4.64-fold), and camel (16.58-fold) ACE2 expressing cells. While there was a significant decrease in mink ACE2 expressing cells, no significant change was observed in horse ACE2 compared to human ACE2 (Fig. 2B). None of the tested pseudoviruses showed entry capabilities into CRFK cells lacking exogenous ACE2.

Protease activity on the S1/S2 and S2' cleavage sites of S of SARS-CoV, MERS-CoV, and SARS-CoV-2 parental strain and Omicron subvariants

The S1/S2 and S2' cleavage sites of SARS-CoV, MERS-CoV, and SARS-CoV-2 parental and select Omicron variants are shown in Fig. 3A, with the basic residues near each cleavage site highlighted in yellow. Western Blot analysis (Fig. 3B) was performed to assess processing of the S1/S2 cleavage site of SARS-CoV, MERS-CoV, and SARS-CoV-2 parental strain and Omicron subvariants BA.1.1, BA.4/5, JN.1, and XBB.1 spike protein using concentrated pseudoviruses. Band sizes of approximately 180 or 100 kDa correspond to full-length, uncleaved S or cleaved S2 domain, respectively. While SARS-CoV S remained primarily unprocessed, a majority of MERS-CoV S were processed prior to release from the parental cell, consistent with the presence or absence of the multibasic cleavage site at S1/S2 in MERS-CoV S and SARS-CoV S respectively. Interestingly, while SARS-CoV-2 contained a multibasic cleavage site promoting S1/S2 processing by host furin, only approximately half of parental SARS-CoV-2 S was processed, whereas a majority of the Omicron subvariants were almost entirely cleaved.

To understand the differences in TMPRSS2 processing of these various S, HEK293T cells expressing human ACE2 (or DPP4 for MERS-CoV pseudoviruses) with and without TMPRSS2 were transduced with pseudoviruses carrying S of SARS-CoV, MERS-CoV, or SARS-CoV-2 parental strain and Omicron subvariants BA.1.1, BA.4/5, JN.1, and XBB.1 (Fig. 3C). The entry of all pseudoviruses assessed significantly increased in the presence of TMPRSS2, though at varying levels. The presence of TMPRSS2 was shown to significantly increase SARS-CoV by approximately 10-fold, MERS-CoV by approximately 46-fold, SARS-CoV-2 parental strain by approximately 34-fold, and Omicron subvariants BA.1 by approximately 181-fold, BA.4/5 by approximately 35-fold, JN.1 by approximately 232-fold, and XBB.1 by approximately 108-fold. None of the tested pseudoviruses showed entry into HEK293T cells lacking exogenous ACE2 or DPP4.

In addition to entry studies, fusion assays were performed using S of parental SARS-CoV-2, SARS-CoV, and MERS-CoV (Fig. 4A). HEK293T cells co-transfected with S from parental SARS-CoV-2, SARS-CoV, or MERS-CoV and their functional receptor with or without TMPRSS2 were used to assess the fusion capabilities of each S. The numbers of nuclei involved in syncytia formation per 20x view was counted over five different fields of view and averaged for the comparative analysis. In cells co-transfected with parental S of SARS-CoV-2 or SARS-CoV with ACE2 alone, expression of both proteins resulted in efficient syncytia formation with counted nuclei at an average of 32.5 and 20.8 respectively. For cells co-transfected with S of MERS-CoV and DPP4, little fusion was observed with an average of 2.8 nuclei in syncytia formation. When these cells also expressed TMPRSS2, the average numbers of nuclei in syncytia per field were significantly increased for SARS-CoV-2 (70.6 nuclei), SARS-CoV (65.4 nuclei), or MERS-CoV S (10.8 nuclei). Representative fusion images can be seen in Fig. 4B.

Effects of cathepsin L inhibitors on the entry of Omicron strains compared to parental strain in the pseudotype virus assay

In the absence of TMPRSS2, SARS-CoV-2 enters the cell through an endosomal route and S is processed by host cathepsins, primarily Cathepsin L. Both MDL28170 and Z-FL-CHO were highly potent against cathepsin L with IC_{50}, 0.01 or 0.015 μM in the enzyme assay, respectively (Table 2). In the virus entry assay, while both inhibited

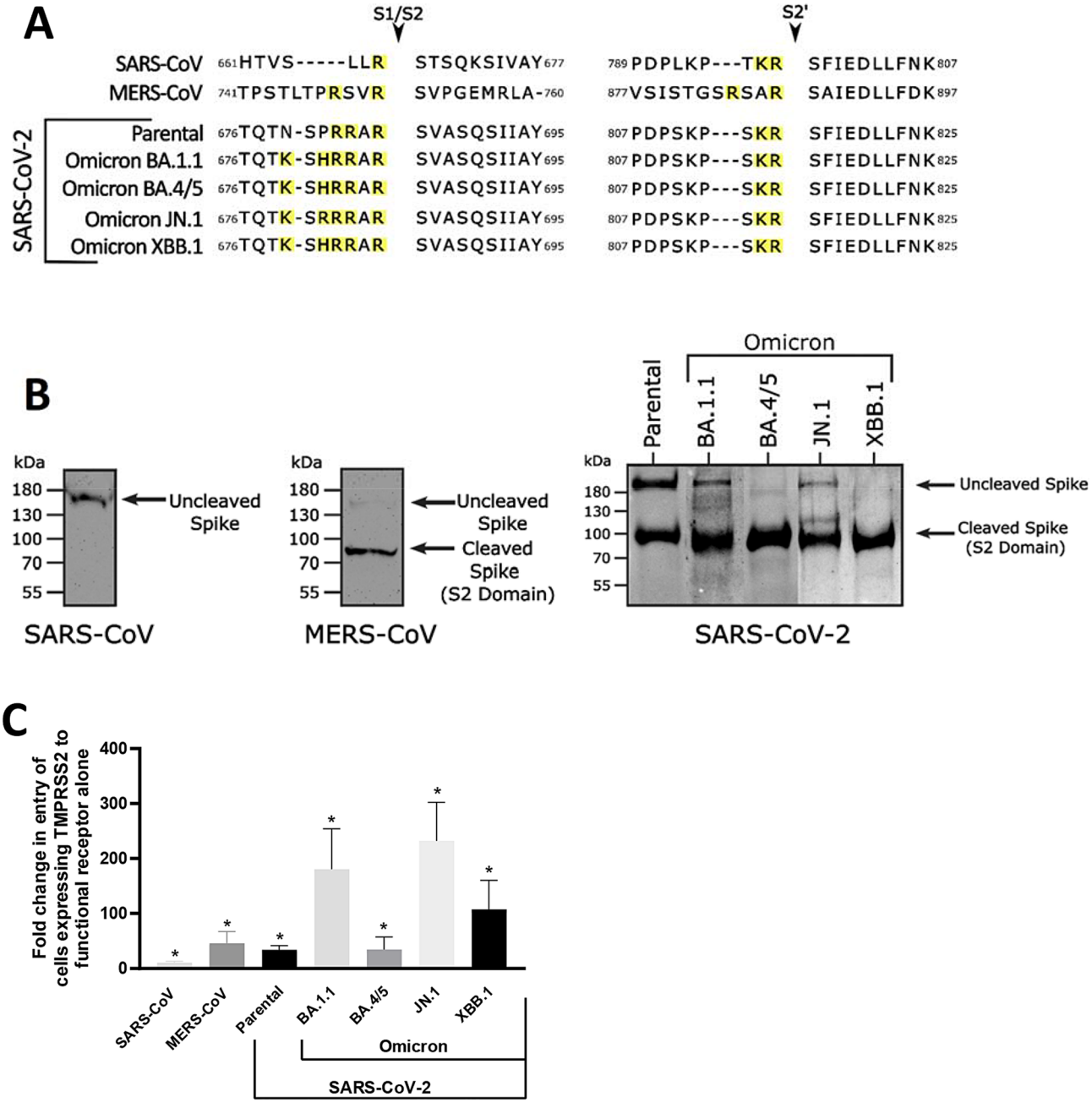

Fig. 3 Protease activity against S of SARS-CoV, MERS-CoV, and SARS-CoV-2 parental and Omicron subvariants BA.1.1, BA.4/5, JN.1, and XBB.1. (**A**) Sequences of the S1/S2 junction and S2′ cleavage site of S from SARS-CoV, MERS-CoV, and SARS-CoV-2 parental and Omicron BA.1.1, BA.4/5, JN.1, and XBB.1. Basic residues near each cleavage sight are shown in yellow highlights. (**B**) Western blot analysis of S cleavage from concentrated pseudoviruses. (**C**) The entry of pseudoviruses expressing S of SARS-CoV and SARS-CoV-2 (parental and Omicron subvariants) into cells expressing the functional receptor ACE2 with or without TMPRSS2, and the entry of pseudoviruses expressing MERS-CoV S into cells expressing the functional receptor DPP4 with or without TMPRSS2. Asterisks show statistical differences ($p < 0.05$) of the entry in the presence of TMPRSS2

the entry of pseudotyped viruses carrying S from parental or omicron SARS-CoV-2, there was greater inhibition against parental compared to omicron strains (>10-fold, $p < 0.01$) (Table 2). The EC_{50} of MDL28170 against parental SARS-CoV-2 was approximately 0.017 μM, while the EC_{50} for BA.1.1, BA.4/5, JN.1, and XBB.1 was approximately 0.36, 0.34, 0.30, and 0.36 μM, respectively. Similarly, the EC_{50} of Z-FL-CHO against SARS-CoV-2 was approximately 0.023, while the EC_{50} of BA1.1, BA.4/5, JN.1, and XBB was 0.34, 0.41, 0.37, and 0.42, respectively.

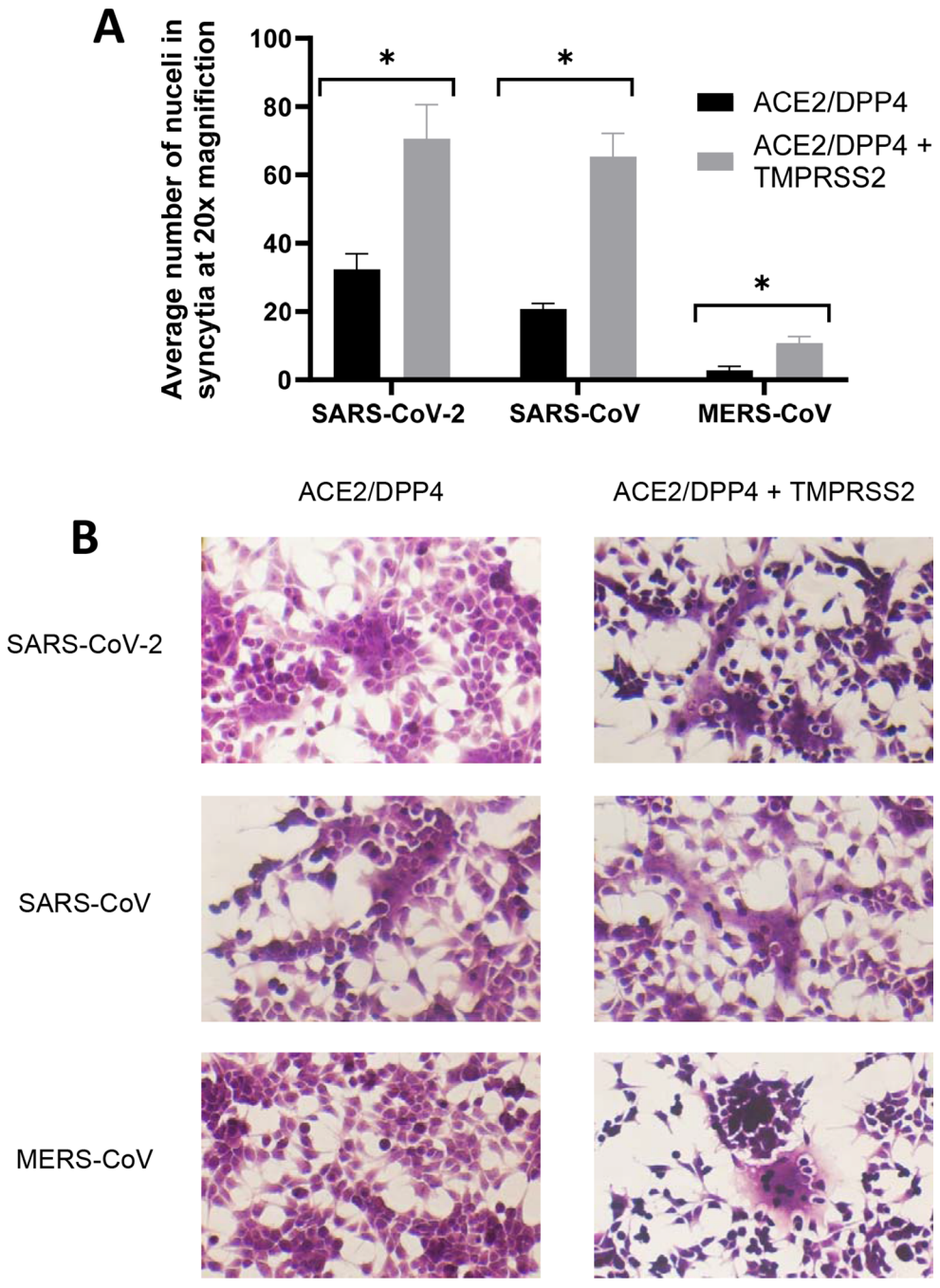

Fig. 4 Fusion assay results. (**A**) The average numbers of nuclei in syncytia per 20x field are shown for parental S of SARS-CoV-2, SARS-CoV, and MERS-CoV. (**B**) Representative fusion images with the H&E stain after co-transfection with S from SARS-CoV-2, SARS-CoV, or MERS-CoV and ACE2/DPP4 with or without TMPRSS2 shown at 40x magnification. Asterisks show statistical differences ($p < 0.05$) of the number of nuclei in syncytia per 20x field when TMPRSS2 is present

Table 2 Effects of cathepsin L inhibitors on the entry Omicron strains in the pseudotype virus assay expressing S

	EC_{50} (μM) Virus entry assay					IC_{50} (μM) Enzyme assay
	Parental Wu	**BA.4/5**	**XBB**	**JN.1**	**B.1.1**	**Cath L**
MDL28170	0.017 ± 0.16	0.34 ± 0.13*	0.36 ± 0.05*	0.30 ± 0.03*	0.36 ± 0.01*	0.01 ± 0.03
Z-FL-CHO	0.023 ± 0.01	0.41 ± 0.04*	0.42 ± 0.01*	0.37 ± 0.02*	0.34 ± 0.04*	0.015 ± 0.02

Numbers are mean ± SD of three independent results. * $p < 0.05$

Discussion

Previous research using pseudoviruses carrying S of SARS-CoV-2 and cells expressing human or animal ACE2 has revealed that several mutations in the RBD in variant strains can alter viral entry [36–38]. Omicron variants have accumulated more mutations throughout of the genome including S (Table 1) compared prior variant types. Many studies have been focused on the biological relevance of the mutations influencing the receptor bindings. It was shown that some mutations in S of Omicron variants including K417N (BA.1.1, BA.4/5 and JN.1), G446S (BA.1.1), E484A (BA.1.1 and BA.4/5), G496S (BA.1.1), and Y505H (BA.1.1, BA.4/5 and JN.) were associated with decreased binding affinity to human ACE2, while mutations such as S477N (BA.1.1, BA.4/5 and JN.1), and N501Y (BA.1.1, BA.4/5 and JN.1) increased the binding affinity in a compensatory manner [39]. In addition, an increase in the amount of positively charged amino acids in the RBD of Omicron variants has been found to decrease the stability of S trimer in the closed position, causing them to adopt an open position more frequently than the parental strain [21, 40]. It was also shown that although K417N mutation conserved in the Omicron variants decreases a binding efficiency to ACE2, it increases the stability of an open conformation which overall contributes to effective binding [41].

We have previously reported the entry of pseudoviruses carrying S of SARS-CoV-2 parental strain and variants of concern (VOC) including alpha, beta and delta variants into cells expressing human or animal (domestic and wild) ACE2 [30]. In this study, we extended to the studies with S from Omicron variants including BA.1.1, BA.4/5, JN.1, and XBB.1. The results showed that the overall entry patterns to cells expressing each animal ACE2 of Omicron BA.4/5 and XBB.1 were similar to each other and to parental strain (Fig. 1A, C and E). In addition, overall entry patterns to cells expressing each animal ACE2 of Omicron BA1.1 and JN.1 were similar to each other (Fig. 1B and D). Among the cells expressing animal ACE2, cow and camel ACE2 were efficiently mediated the entries of all tested Omicron strains compared to human ACE2 (Fig. 1B-E). On the other hand, the entries of all tested Omicron strains were decreased to mink ACE2 compared human ACE2 (Fig. 1B-E). This is consistent with our lab's previous work [30] as well as a report from Damas et al. [42] predicting weak binding of SARS-CoV-2 S to mink ACE2 using in silico analysis. It is not clear why there is the discrepancy between natural infections in minks and poor entry with mink ACE2. It is possible that additional host proteins are required for efficient entry for minks. There were variable entry efficiencies into cells expressing horse, dog, cat, hamster and WTD ACE2 among Omicron strains (Fig. 1B-E). Li et al. [37] reported that S of Omicron BA.1 and BA.2 enhanced binding and entry efficiency with some animal ACE2, including rodents and bats, suggesting a potentially extended host range. The S of BA.4/5 are closely related to BA.2 with two additional substitutions in the RBD (L452R and F486V) and a 493Q that is a mutation reverted to the parental strain. Additional studies [37, 38, 43] showed that that Omicron BA.1, BA.2 and BA.3 have higher binding capacity to many animal ACE2 or increased entry compared to the parental strain using the pseudoviruses carrying S. Regarding BA.4/5, a binding assay study [38] showed that BA.4/5 share similar enhanced binding affinity to many animal ACE2 with BA.1–3. Motozono et al. [44] reported that S of BA.4/5 variant had increased stability in the open conformation by the L452R mutation which is not present in BA.1.1 or JN.1., and this may be the reason for increase of entries to cells expressing most of tested animal ACE2 in this study (Fig. 1C). There were efficient entries of the most pseudoviruses carrying parental or Omicron strain into cells expressing cow and horse ACE2, the species showing limited evidence of virus infection in vivo [45–52] suggesting there might be additional factors involved in viral replication and pathogenicity.

Both SARS-CoV and SARS-CoV-2 use ACE2 as the receptor for successful viral entry and infection. Since the last known human SARS-CoV cases in 2004, its zoonotic potential was studied with wild animals found at the live market in China, including palm civets (*Paguma larvata*), raccoon dogs (*Nyctereutes procyonoides*), and ferret badgers (*Melogale*) [53], and domestic species including cats and ferrets [54, 55]. Using the entry assay with cells expressing human or animal ACE2, we found that pseudoviruses carrying S of SARS-CoV entered the cells at efficiency comparable to those of SARS-CoV-2 (parental) in most tested cells (Fig. 2A and B). SARS-CoV and SARS-CoV-2 are *Sarbecoviruses* that use ACE2 as a cellular receptor and have a 75% amino acid homology in their S [56], thus it is not surprising that they have similar ACE2 bindings and entry capacities. It would be interesting to see whether this host susceptibility trend could be extended to other members of *Sarbecoviruses* that utilize ACE2 as a receptor. Our results indicated an efficient entry ability in many animal ACE2 expressing cells such as hamster, cat, and white-tailed deer, all of which have been shown to harbor natural infections (Supplementary Table 1).

ACE2 is the receptor molecule that is indispensable for SARS-CoV-2 and SARS-CoV infection, whereas DPP4 is the necessary receptor molecule for MERS-CoV. It is believed that sequential proteolytic processing at the S1/S2 junction in the parental cell and the S2' cleavage site in the target cell is required for virus entry. Both S of SARS-CoV-2 and MERS-CoV contain polybasic amino acids at the S1/S2 junction (RRXR and RXXR, respectively), but

SARS-CoV has a single Arg (Fig. 3A). The presence of polybasic residues at the S1/S2 junction is shown to allow processing by a wider range of cellular proteases such as furin, which efficiently cleave R-X-(R/K/X)-R sequence [57], and it was reported that furin efficiently cleaves the S1/S2 junction of S of SARS-CoV-2 [58, 59] and MERS-CoV [60]. In our Western blot analysis, about half of S of SARS-CoV-2 parental strain pseudoviruses from HEK293T cells were proteolytically processed, yielding an uncleaved band and a cleaved band that corresponds to the S2 domain (Fig. 3B). While the parental SARS-CoV-2 S was only approximately 50% cleaved, the Omicron subvariants were almost entirely cleaved (Fig. 3B). All Omicron spike proteins tested contain the mutations N679K and either P681H (BA.1.1, BA.4/5, XBB.1) or P681R (JN.1). These mutations create additional basic residues at the multibasic furin cleavage site (Fig. 3A). The P681H found in the Alpha and Mu variants as well as the P681R mutation found in the Delta variant have been found to increase processing at the S1/S2 site, with more cleavages with the mutation of P681R than P681H [61–63]. Additionally, the N679K mutation has also been attributed to more cleavages by furin in fluorogenic cleavage assays, lending to improved cleavage of S1/S2 compared to previous variants only containing a mutation at P681 [64]. Similar to the Omicron subvariants, MERS-CoV S, which also contains a multibasic sequence at S1/S2, was majorly processed. Interestingly, though there are less basic resides at the S1/S2 cleavage site than the parental SARS-CoV-2 S, MERS-CoV-S appeared to be majorly cleaved (Fig. 3B). In contrast, the majority of S of SARS-CoV remained intact (Fig. 3B), as SARS-CoV S lacks the residues necessary for furin processing, which is consistent with previous reports [65, 66].

While the processing of S1/S2 occurs in the infected cells prior to release, it is believed that following the binding of SARS-CoV, MERS-CoV, and SARS-CoV-2 to their respective functional receptor, these coronaviruses can utilize TMPRSS2-mediated entry via fusion at the cell membrane or endosomal pathway in TMPRSS2-negative cells [27, 65]. It is speculated that furin-mediated cleavage of the S1/S2 junction works in concert with TMPRSS2 to promote viral entry [59, 67]. The aim of our study was to understand the extent to which TMPRSS2 acts on S of these coronaviruses in comparison to one another using HEK293T cells expressing ACE2 for SARS-CoV and SARS-CoV-2 and DPP4 for MERS-CoV with or without TMPRSS2. As expected, entry of these coronaviruses all significantly increased when TMPRSS2 was expressed, though at varying magnitudes. Consistent with the speculation that TMPRSS2 works in conjunction with furin cleavage, SARS-CoV, which is majorly uncleaved at S1/S1 (Fig. 3B), had the lowest fold increase in entry (10-fold) with TMPRSS2 expression (Fig. 3C). SARS-CoV-2 parental strain, in which only approximately 50% of S is cleaved (Fig. 3B), had a moderate increase in fold change when TMPRSS2 was expressed (34-fold) as opposed to when only ACE2 was expressed (Fig. 2C). The spike proteins of MERS-CoV and SARS-CoV-2 Omicron BA.1.1, BA.4/5, JN.1, and XBB.1 were all majorly cleaved at S1/S2 in the parental cell (Fig. 3B). Interestingly, while Omicron BA.1.1, JN.1, and XBB.1 pseudoviruses showed a marked increase in entry with the presence of TMRSS2 (181-fold, 232-fold, and 108-fold respectively), the increase in entry for MERS-CoV and SARS-CoV-2 Omicron BA.4/5 was more moderate (46-fold and 35-fold respectively) (Fig. 3C).

Fusogenicity is implicated in virulence and immune evasion of coronaviruses, and the ability of SARS-CoV, SARS-CoV-2, and MERS-CoV S to mediate cell-to-cell fusion has been independently demonstrated both in vitro and in vivo [68]. TMPRSS2 expression has been linked to viral-induced syncytia formation, which is thought to contribute to viral pathogenicity in vivo. Infected syncytia is a common pathological finding in lung tissues of patients infected with SARS-CoV-2 [69]. When Iwata-Yoshikawa et al. [70] inoculated TMPRSS2 knockout mice with various strains of SARS-CoV-2, they showed significant reduction in viral load and pathological lung changes compared to their wild-type counterparts. Additionally, they found the use of TMPRSS2 inhibitor Nafamostat significantly reduced the viral infectivity in vivo. Hampering both the direct membrane fusion entry route and the cell-to-cell transmission that would occur during fusion events makes TMPRSS2 inhibitors an attractive therapy for SARS-CoV-2 treatment. Our goal in this study was to comparatively assess the utilization of TMPRSS2 in S fusogenicity of SARS-CoV, SARS-CoV-2, and MERS-CoV in relation to each other, and to our entry study. To study this, we co-transfected each S and respective receptor with or without TMPRSS2. In agreement with the entry studies, in the presence of TMPRSS2, more syncytia were formed by S of SARS-CoV-2, SARS-CoV, and MERS-CoV. The S of SARS-CoV-2 or SARS-CoV resulted in more robust syncytia formation than S of MERS-CoV with or without TMPRSS2 (Fig. 4A). Less Synthia formation by S of MERS-CoV may be due to the usage of different receptor from S of SARS-CoV/SARS-CoV-2.

There are numerous evidences [71, 72] showing SARS-CoV-2 Omicron strains are more infectious with the improved binding to ACE2 [73], and less virulent [71, 72] compared to earlier strains. Some early studies showed that SARS-CoV-2 Omicron strains were less likely rely on TMPRSS2 than parental strain for viral entry [73, 74]. Peacock et al. [63] showed that SARS-CoV-2 Omicron strains were found to replicate efficiently in nasal epithelium, which lacks TMPRSS2. However, other studies

showed the important role of TMPRSS2 for Omicron strains in vitro [75] and in vivo [70, 76]. In TMPRSS2 knockout animals, the infection of SARS-CoV-2 Omicron strain resulted in severe loss of infection and pathogenicity [70, 76]. Regarding endosome-mediated entry of Omicron strains, Sakurai et al. [77] reported SARS-CoV-2 Omicron variant progressively adapted to use the endosome route by comparing the inhibitory activity of E64d (cathepsin L inhibitor) between a Delta strain and several Omicron strains. In this study, we used two cathepsin L inhibitors to examine their effects on virus entry. There were significant differences (greater than ten-fold) in EC_{50} of MDL28170 and Z-FL-CHO against Omicron strains compared to parental strain (Table 2), suggesting Omicron strains do not depend on the endosomal route compared to parental strain. It is possible that more efficient S1/S2 cleavage of Omicron strains than parental strain (Fig. 3B) resulted in increased EC_{50} values. The differences between ours from Sakurai's results may be due to using different pseudoviruses, SARS-CoV-2 strains, cell types, and cathepsin L inhibitors.

Though the pseudovirus system is a safe and fast method for virus analysis with wide applications, it is not without limitations. While this system is good for assessing the entry capability of a virus, it cannot assess the replication efficiency. Both SARS-CoV and SARS-CoV-2 have demonstrated the ability to enter, but not replicate in various human and animal cell lines [78]. Therefore, this assay should be validated using live viruses. Additionally, we used cells exogenously expressing ACE2, DPP4 and TMPRSS2, which may lack endogenous proteins that aid or inhibit viral entry that may be present in cells naturally susceptible to the tested coronaviruses.

In summary, our results suggest the importance of continual evaluation of SARS-CoV-2 variants in their susceptibility to animal species, as well as monitoring entry routes and performing inhibitor screening of emerging strains. Comparable analysis of entry efficacies of SARS-CoV-2 variants as well as SARS-CoV and MERS-CoV provides detailed information regarding entry processes among different coronaviruses.

Abbreviations

ACE2	Angiotensin-Converting Enzyme 2
COVID-19	Coronavirus Disease of 2019
CRFK	Crandell-Rees Feline Kidney (cell line)
DMEM	Dulbecco's Modified Eagle Medium
DPP4	Dipeptidyl Peptidase-4
HEK293T	Human Embryonic Kidney 293T (cell line)
MEM	Eagle's Minimal Essential Medium
MERS-CoV	Middle Eastern Respiratory Syndrome Coronavirus
RBD	Receptor Binding Domain
S	Spike Protein
SARS-CoV	Severe Acute Respiratory Syndrome Coronavirus
SARS-CoV-2	Severe Acute Respiratory Syndrome Coronavirus 2
TMRSS2	Transmembrane Serine Protease 2

Supplementary Information

The online version contains supplementary material available at https://doi.org/10.1186/s12917-025-04822-9.

Supplementary Material 1

Supplementary Material 2

Acknowledgements

The authors thank David George for technical assistance.

Author contributions

KOC and YK conceived the idea of the study, and KOC, YK and AZ participated in its flow and coordinated the draft of the manuscript. All authors read and approved the final manuscript. KOC, YK and AZ performed and analyzed experiments including cell-based assays.

Funding

National Institutes of Health (NIH) (grants R01 AI130092 and AI161085).

Data availability

Availability of data and materialThe data that support the findings of this study are available on request from the corresponding author (KOC).

Declarations

Ethics approval and consent to participate

Not applicable.

Consent for publication

Not applicable.

Competing interests

The authors declare no competing interests.

Received: 17 February 2025 / Accepted: 9 May 2025
Published online: 27 May 2025

References

1. Sørensen MD, Sørensen B, Gonzalez-Dosal R, Melchjorsen CJ, Weibel J, Wang J, et al. Severe acute respiratory syndrome (SARS): development of diagnostics and antivirals. Ann N Y Acad Sci. 2006;1067(1):500–5.
2. C.D.C. CDC SARS Response Timeline| About| CDC. 2021.
3. C.D.C. Middle East Respiratory Syndrome / MERS| CDC Yellow Book 2024 2023 [Available from: https://wwwnc.cdc.gov/travel/yellowbook/2024/infections-diseases/mers
4. W.H.O. Middle East respiratory syndrome coronavirus (MERS-CoV) [Available from: https://www.who.int/health-topics/middle-east-respiratory-syndrome-coronavirus-mers#tab=tab_2
5. W.H.O. Middle East respiratory syndrome: global summary and assessment of risk 2022 [.
6. Pormohammad A, Ghorbani S, Khatami A, Farzi R, Baradaran B, Turner DL, et al. Comparison of confirmed COVID-19 with SARS and MERS cases - Clinical characteristics, laboratory findings, radiographic signs and outcomes: A systematic review and meta-analysis. Rev Med Virol. 2020;30(4):e2112.
7. Huang C, Wang Y, Li X, Ren L, Zhao J, Hu Y, et al. Clinical features of patients infected with 2019 novel coronavirus in Wuhan, China. Lancet. 2020;395(10223):497–506.
8. Ma Q, Liu J, Liu Q, Kang L, Liu R, Jing W, et al. Global percentage of asymptomatic SARS-CoV-2 infections among the tested population and individuals with confirmed COVID-19 diagnosis: A systematic review and Meta-analysis. JAMA Netw Open. 2021;4(12):e2137257–e.
9. Symptoms CDC. 2022 [Available from: https://www.cdc.gov/coronavirus/2019-ncov/symptoms-testing/symptoms.html
10. Ou J, Lan W, Wu X, Zhao T, Duan B, Yang P, et al. Tracking SARS-CoV-2 Omicron diverse Spike gene mutations identifies multiple inter-variant recombination events. Signal Transduct Target Ther. 2022;7(1):138.

11. Tegally H, Wilkinson E, Lessells RJ, Giandhari J, Pillay S, Msomi N, et al. Sixteen novel lineages of SARS-CoV-2 in South Africa. Nat Med. 2021;27(3):440–6.
12. Dhawan M, Saied AA, Mitra S, Alhumaydhi FA, Emran TB, Wilairatana P. Omicron variant (B.1.1.529) and its sublineages: what do we know so Far amid the emergence of Recombinant variants of SARS-CoV-2? Biomed Pharmacother. 2022;154:113522.
13. Tracking WHO. SARS-CoV-2 variants 2023 [Available from: https://www.who.int/activities/tracking-SARS-CoV-2-variants
14. Orgnization WH. Updated Risk Evaluation of JN.1, 15 April 2024. 2024.
15. Khare S, Gurry C, Freitas L, Schultz MB, Bach G, Diallo A, et al. GISAID's role in pandemic response. China CDC Wkly. 2021;3(49):1049–51.
16. Gangavarapu K, Latif AA, Mullen JL, Alkuzweny M, Hufbauer E, Tsueng G, et al. Outbreak.info genomic reports: scalable and dynamic surveillance of SARS-CoV-2 variants and mutations. Nat Methods. 2023;20(4):512–22.
17. Prevention CfDCa. COVID Data Tracker Atlanta, GA: U.S: Department of Health and Human Services, CDC. 2025 [Available from: https://covid.cdc.gov/covid-data-tracker
18. Zabiegala A, Kim Y, Chang KO. Roles of host proteases in the entry of SARS-CoV-2. Anim Dis. 2023;3(1):12.
19. Berger I, Schaffitzel C. The SARS-CoV-2 Spike protein: balancing stability and infectivity. Cell Res. 2020;30(12):1059–60.
20. Costello SM, Shoemaker SR, Hobbs HT, Nguyen AW, Hsieh C-L, Maynard JA, et al. The SARS-CoV-2 Spike reversibly samples an open-trimer conformation exposing novel epitopes. Nat Struct Mol Biol. 2022;29(3):229–38.
21. Mori T, Jung J, Kobayashi C, Dokainish HM, Re S, Sugita Y. Elucidation of interactions regulating conformational stability and dynamics of SARS-CoV-2 S-protein. Biophys J. 2021;120(6):1060–71.
22. Perlman S, Masters PS. Coronaviridae:The viruses and their replication. In: M.Howley P, M.Knipe D, Whelan S, editors. Fields virology:emerging viruses. 7th ed. Philadelphia: Lippincott Williams & Wilkens; 2020.
23. Gallagher TM, Buchmeier MJ. Coronavirus Spike proteins in viral entry and pathogenesis. Virology. 2001;279(2):371–4.
24. Millet JK, Whittaker GR. Host cell entry of middle East respiratory syndrome coronavirus after two-step, furin-mediated activation of the Spike protein. Proc Natl Acad Sci U S A. 2014;111(42):15214–9.
25. Bestle D, Heindl MR, Limburg H, Van Lam T, Pilgram O, Moulton H et al. TMPRSS2 and Furin are both essential for proteolytic activation of SARS-CoV-2 in human airway cells. Life Sci Alliance. 2020;3(9).
26. Papa G, Mallery DL, Albecka A, Welch LG, Cattin-Ortolá J, Luptak J, et al. Furin cleavage of SARS-CoV-2 Spike promotes but is not essential for infection and cell-cell fusion. PLoS Pathog. 2021;17(1):e1009246.
27. Koch J, Uckeley ZM, Doldan P, Stanifer M, Boulant S, Lozach PY. TMPRSS2 expression dictates the entry route used by SARS-CoV-2 to infect host cells. Embo J. 2021;40(16):e107821.
28. Matsuyama S, Ujike M, Morikawa S, Tashiro M, Taguchi F. Protease-mediated enhancement of severe acute respiratory syndrome coronavirus infection. Proc Natl Acad Sci U S A. 2005;102(35):12543–7.
29. Hoffmann M. HH-W, S Pöhlmann. How cellular proteases arm coronavirus Spike proteins. Springer International Publishing AG; 2018. pp. 71–98.
30. Kim Y, Gaudreault NN, Meekins DA, Perera KD, Bold D, Trujillo JD et al. Effects of Spike mutations in SARS-CoV-2 variants of concern on human or animal ACE2-Mediated virus entry and neutralization. Microbiol Spectr. 2022:e0178921.
31. Jawad B, Adhikari P, Podgornik R, Ching W-Y. Key interacting residues between RBD of SARS-CoV-2 and ACE2 receptor: combination of molecular dynamics simulation and density functional calculation. J Chem Inf Model. 2021;61(9):4425–41.
32. Borkotoky S, Dey D, Hazarika Z. Interactions of angiotensin-converting enzyme-2 (ACE2) and SARS-CoV-2 Spike receptor-binding domain (RBD): a structural perspective. Mol Biol Rep. 2023;50(3):2713–21.
33. University S. Stanford Coronavirus Antiviral & Resistance Database (CoVDB) 2024 [Available from: https://covdb.stanford.edu/
34. Dampalla CS, Nguyen HN, Rathnayake AD, Kim Y, Perera KD, Madden TK, et al. Broad-Spectrum Cyclopropane-Based inhibitors of coronavirus 3 C-like proteases: biochemical, structural, and virological studies. ACS Pharmacol Transl Sci. 2023;6(1):181–94.
35. Li P, Kim Y, Dampalla CS, Nhat Nguyen H, Meyerholz DK, Johnson DK, et al. Potent 3CLpro inhibitors effective against SARS-CoV-2 and MERS-CoV in animal models by therapeutic treatment. mBio. 2024;15(2):e0287823.
36. Han P, Li L, Liu S, Wang Q, Zhang D, Xu Z, et al. Receptor binding and complex structures of human ACE2 to Spike RBD from Omicron and delta SARS-CoV-2. Cell. 2022;185(4):630–40. e10.
37. Li L, Han P, Huang B, Xie Y, Li W, Zhang D, et al. Broader-species receptor binding and structural bases of Omicron SARS-CoV-2 to both mouse and palm-civet ACE2s. Cell Discov. 2022;8(1):65.
38. Zhao Z, Xie Y, Bai B, Luo C, Zhou J, Li W, et al. Structural basis for receptor binding and broader interspecies receptor recognition of currently Circulating Omicron sub-variants. Nat Commun. 2023;14(1):4405.
39. Han P, Li L, Liu S, Wang Q, Zhang D, Xu Z, et al. Receptor binding and complex structures of human ACE2 to Spike RBD from Omicron and delta SARS-CoV-2. Cell. 2022;185(4):630–e4010.
40. Yin W, Xu Y, Xu P, Cao X, Wu C, Gu C et al. Structures of the Omicron Spike trimer with ACE2 and an anti-Omicron antibody: mechanisms for the high infectivity, immune evasion and antibody drug discovery. BioRxiv. 2021:2021.12.27.474273.
41. Wrobel AG, Benton DJ, Roustan C, Borg A, Hussain S, Martin SR, et al. Evolution of the SARS-CoV-2 Spike protein in the human host. Nat Commun. 2022;13(1):1178.
42. Damas J, Hughes GM, Keough KC, Painter CA, Persky NS, Corbo M, et al. Broad host range of SARS-CoV-2 predicted by comparative and structural analysis of ACE2 in vertebrates. Proc Natl Acad Sci U S A. 2020;117(36):22311–22.
43. Neerukonda SN, Wang R, Vassell R, Baha H, Lusvarghi S, Liu S, et al. Characterization of entry pathways, Species-Specific Angiotensin-Converting enzyme 2 residues determining entry, and antibody neutralization evasion of Omicron BA.1, BA.1.1, BA.2, and BA.3 variants. J Virol. 2022;96(17):e0114022.
44. Motozono C, Toyoda M, Zahradnik J, Saito A, Nasser H, Tan TS, et al. SARS-CoV-2 Spike L452R variant evades cellular immunity and increases infectivity. Cell Host Microbe. 2021;29(7):1124–e3611.
45. Bosco-Lauth AM, Walker A, Guilbert L, Porter S, Hartwig A, McVicker E, et al. Susceptibility of livestock to SARS-CoV-2 infection. Emerg Microbes Infect. 2021;10(1):2199–201.
46. Cerino P, Buonerba C, Brambilla G, Atripaldi L, Tafuro M, Concilio DD, et al. No detection of SARS-CoV-2 in animals exposed to infected keepers: results of a COVID-19 surveillance program. Future Sci OA. 2021;7(7):Fso711.
47. Ulrich L, Wernike K, Hoffmann D, Mettenleiter TC, Beer M. Experimental infection of cattle with SARS-CoV-2. Emerg Infect Dis. 2020;26(12):2979–81.
48. Falkenberg S, Buckley A, Laverack M, Martins M, Palmer MV, Lager K et al. Experimental inoculation of young calves with SARS-CoV-2. Viruses. 2021;13(3).
49. El Masry I, Al Makhladi S, Al Abdwany M, Al Subhi A, Eltahir H, Cheng S, et al. Serological evidence of SARS-CoV-2 infection in dromedary camels and domestic Bovids in Oman. Emerg Microbes Infect. 2023;12(1):2220577.
50. Hüttl J, Reitt K, Meli ML, Meili T, Bönzli E, Pineroli B et al. Serological and molecular investigation of SARS-CoV-2 in horses and cattle in Switzerland from 2020 to 2022. Viruses. 2024;16(2).
51. Pusterla N, Chaillon A, Ignacio C, Smith DM, Barnum S, Lawton KOY et al. SARS-CoV-2 seroconversion in an adult horse with direct contact to a COVID-19 individual. Viruses. 2022;14(5).
52. Lawton KOY, Arthur RM, Moeller BC, Barnum S, Pusterla N. Investigation of the role of healthy and sick equids in the COVID-19 pandemic through serological and molecular testing. Anim (Basel). 2022;12(5).
53. Kan B, Wang M, Jing H, Xu H, Jiang X, Yan M, et al. Molecular evolution analysis and geographic investigation of severe acute respiratory syndrome coronavirus-like virus in palm civets at an animal market and on farms. J Virol. 2005;79(18):11892–900.
54. Wang M, Jing HQ, Xu HF, Jiang XG, Kan B, Liu QY, et al. [Surveillance on severe acute respiratory syndrome associated coronavirus in animals at a live animal market of Guangzhou in 2004]. Zhonghua Liu Xing Bing Xue Za Zhi. 2005;26(2):84–7.
55. Martina BE, Haagmans BL, Kuiken T, Fouchier RA, Rimmelzwaan GF, Van Amerongen G, et al. Virology: SARS virus infection of cats and ferrets. Nature. 2003;425(6961):915.
56. Zhou P, Yang XL, Wang XG, Hu B, Zhang L, Zhang W, et al. A pneumonia outbreak associated with a new coronavirus of probable Bat origin. Nature. 2020;579(7798):270–3.
57. Thomas G. Furin at the cutting edge: from protein traffic to embryogenesis and disease. Nat Rev Mol Cell Bio. 2002;3(10):753–66.
58. Bestle D, Heindl MR, Limburg H, Van TVL, Pilgram O, Moulton H et al. TMPRSS2 and Furin are both essential for proteolytic activation of SARS-CoV-2 in human airway cells. Life Sci Alliance. 2020;3(9).
59. Essalmani R, Jain J, Susan-Resiga D, Andreo U, Evagelidis A, Derbali RM, et al. Distinctive roles of Furin and TMPRSS2 in SARS-CoV-2 infectivity. J Virol. 2022;96(8):e0012822.

60. Kleine-Weber H, Elzayat MT, Hoffmann M, Pöhlmann S. Functional analysis of potential cleavage sites in the MERS-coronavirus Spike protein. Sci Rep. 2018;8(1):16597.
61. Ke Z, Peacock TP, Brown JC, Sheppard CM, Croll TI, Kotecha A, et al. Virion morphology and on-virus Spike protein structures of diverse SARS-CoV-2 variants. EMBO J. 2024;43(24):6469–95.
62. Saito A, Irie T, Suzuki R, Maemura T, Nasser H, Uriu K, et al. Enhanced fusogenicity and pathogenicity of SARS-CoV-2 Delta P681R mutation. Nature. 2022;602(7896):300–6.
63. Liu Y, Liu J, Johnson BA, Xia H, Ku Z, Schindewolf C, et al. Delta Spike P681R mutation enhances SARS-CoV-2 fitness over alpha variant. Cell Rep. 2022;39(7):110829.
64. Lubinski B, Jaimes JA, Whittaker GR. Intrinsic furin-mediated cleavability of the Spike S1/S2 site from SARS-CoV-2 variant B.1.1.529 (Omicron). BioRxiv. 2022.
65. Hoffmann M, Kleine-Weber H, Schroeder S, Krüger N, Herrler T, Erichsen S, et al. SARS-CoV-2 cell entry depends on ACE2 and TMPRSS2 and is blocked by a clinically proven protease inhibitor. Cell. 2020;181(2):271–e808.
66. Belouzard S, Chu VC, Whittaker GR. Activation of the SARS coronavirus Spike protein via sequential proteolytic cleavage at two distinct sites. Proc Natl Acad Sci U S A. 2009;106(14):5871–6.
67. Park JE, Li K, Barlan A, Fehr AR, Perlman S, McCray PB Jr., et al. Proteolytic processing of middle East respiratory syndrome coronavirus spikes expands virus tropism. Proc Natl Acad Sci U S A. 2016;113(43):12262–7.
68. Leroy H, Han M, Woottum M, Bracq L, Bouchet J, Xie M et al. Virus-Mediated Cell-Cell fusion. Int J Mol Sci. 2020;21(24).
69. Lin L, Li Q, Wang Y, Shi Y. Syncytia formation during SARS-CoV-2 lung infection: a disastrous unity to eliminate lymphocytes. Cell Death Differ. 2021;28(6):2019–21.
70. Iwata-Yoshikawa N, Kakizaki M, Shiwa-Sudo N, Okura T, Tahara M, Fukushi S, et al. Essential role of TMPRSS2 in SARS-CoV-2 infection in murine airways. Nat Commun. 2022;13(1):6100.
71. Bálint G, Vörös-Horváth B, Széchenyi A. Omicron: increased transmissibility and decreased pathogenicity. Signal Transduct Target Therapy. 2022;7(1):151.
72. Tamura T, Yamasoba D, Oda Y, Ito J, Kamasaki T, Nao N, et al. Comparative pathogenicity of SARS-CoV-2 Omicron subvariants including BA.1, BA.2, and BA.5. Commun Biology. 2023;6(1):772.
73. Meng B, Abdullahi A, Ferreira IATM, Goonawardane N, Saito A, Kimura I, et al. Altered TMPRSS2 usage by SARS-CoV-2 Omicron impacts infectivity and fusogenicity. Nature. 2022;603(7902):706–14.
74. Aggarwal A, Akerman A, Milogiannakis V, Silva MR, Walker G, Stella AO et al. SARS-CoV-2 Omicron BA.5: evolving tropism and evasion of potent humoral responses and resistance to clinical immunotherapeutics relative to viral variants of concern. eBioMedicine. 2022;84.
75. Mykytyn AZ, Breugem TI, Geurts MH, Beumer J, Schipper D, van Acker R, et al. SARS-CoV-2 Omicron entry is type II transmembrane Serine protease-mediated in human airway and intestinal organoid models. J Virol. 2023;97(8):e0085123.
76. Metzdorf K, Jacobsen H, Greweling-Pils MC, Hoffmann M, Lüddecke T, Miller F et al. TMPRSS2 is essential for SARS-CoV-2 Beta and Omicron infection. Viruses. 2023;15(2).
77. Sakurai Y, Okada S, Ozeki T, Yoshikawa R, Kinoshita T, Yasuda J. SARS-CoV-2 Omicron subvariants progressively adapt to human cells with altered host cell entry. mSphere. 2024;9(9):e0033824.
78. Chu H, Chan JF, Yuen TT, Shuai H, Yuan S, Wang Y, et al. Comparative tropism, replication kinetics, and cell damage profiling of SARS-CoV-2 and SARS-CoV with implications for clinical manifestations, transmissibility, and laboratory studies of COVID-19: an observational study. Lancet Microbe. 2020;1(1):e14–23.

Publisher's note